Lasers in Manufacturing Conference 2025

The effect of laser emission mode on the cutting of lithium metal as a solid-state battery anode

Pourya Heidari Orojloo[a,*], Pantaleone Barbieri[b], Daniela Fontana[b], Ali Gökhan Demir[a]

[a]*Department of Mechanical Engineering, Politecnico di Milano, Via La Masa 1, 20156 Milan, Italy*
[b]*Comau S.p.A. – E-Mobility Global Competence Center, Via Rivalta 30, 10095 Grugliasco, Italy*

Abstract

Lithium metal as an anode in the solid-state battery is a promising alternative to the intercalation type of anode in the lithium-ion battery. However, cutting of this component mechanically is challenging due to its high surface adhesion, chemical reactivity, and low rigidity. On the other hand, the melting temperature of this material is very low (180 °C) compared to conventional metals, rendering it problematic a stable thermal cutting operation. While the laser is an appealing solution for scaling up the cutting process of lithium metal, the ideal laser type to be used for this operation still requires further attention. Accordingly, this work investigates impact of continuous wave and ns-pulsed laser sources on the cut quality and productivity of 50 µm-thick pure Li sheets. Processing conditions are discussed to address the environmental control issues for reactivity along with the different processing regimes observed.

Keywords: Laser cutting; Lithium metal; Solid-state battery; Anode

1. Introduction

Due to the increasing demand for electrification in recent years, the need for energy storage—particularly lithium-ion batteries (LIBs)—has also risen significantly. As a result, there is growing interest in using digital technologies to scale up the manufacturing process, both at the pilot scale and in giga factories. One critical step in battery manufacturing is the cutting of anode, cathode, and separator rolls. Laser cutting presents a promising alternative to traditional mechanical methods for processing LIB electrodes. Various laser sources can be employed to cut these components effectively (Angeloni et al., 2024; Kriegler et al., 2021; Shin et al., 2024). Recent studies also showed the advantage of using novel temporal emission control modes such as burst mode in ultrafast lasers that improve the cut quality on metallic collectors, polymeric separators, and coated electrode materials (Heidari Orojloo and Demir, 2025, 2024; Orojloo and Demir, 2024).

Given the advantages of solid-state batteries (SSBs) (Thomas et al., 2024) over conventional LIBs, many companies are now exploring scalable manufacturing methods for SSB production. The anodes in SSBs typically consist of lithium metal, either alone or combined with a copper current collector. Fig. 1a and Fig. 1b illustrate a schematic of an SSB with pure lithium metal and lithium metal anode (LMA), respectively. Due to the unique mechanical properties and surface adhesion behaviour of lithium metal when interacting with cutting tools (Jansen et al., 2018), laser cutting appears to be an essential method for processing these materials. A comparison of the thermophysical properties of pure lithium and more conventional materials like copper reveals notable differences (Heidari Orojloo et al., 2025). Lithium has a significantly lower melting point and viscosity compared to copper, while its boiling point is about half that of copper. This implies that copper remains in the liquid phase longer during cutting and, due to its higher fluidity, tends to flow more readily.

Research on laser cutting of pure lithium metal and LMAs is still limited. Only a limited number of studies (Heidari Orojloo et al., 2025; Jansen et al., 2019, 2018; Kriegler et al., 2023, 2022) have examined this process on pure Li and Li coated Cu collectors employing different pulsed lasers (Heidari Orojloo et al., 2025; Kriegler et al., 2023). The limited number of studies is also associated to the high reactivity of Li in ambient conditions. Laser systems operating in a dry room or an equivalent chamber is required that renders exploring different laser solutions more limited. Accordingly, this work provides an

overview of laser microcutting of pure Li sheets with 50 µm thickness in an inert atmosphere comparing continuous wave (CW) and nanosecond pulsed wave (PW) solutions. The work aims to show the main differences between the different processing conditions in terms of material removal and defect formation as well as achievable productivity levels.

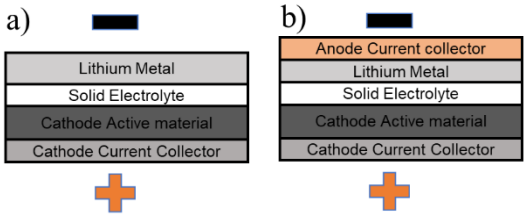

Fig. 1. Graphical schematic of a solid-state battery with (a) pure lithium metal and (b) lithium metal anode.

2. Materials and methods

2.1. Pure lithium metal

The investigations were conducted using commercially available battery-grade pure lithium metal with a thickness of 50 µm. The lithium metal used in this work was of battery-grade quality, with a purity exceeding 99.9%. The anode used corresponds to the pure lithium metal shown in Fig. 1a. The material was received from the supplier in an air-tight pouch filled with argon to prevent chemical degradation. Prior to any experiments, the pure lithium metal was open and stored in a glovebox containing an argon atmosphere with humidity and oxygen levels below 1.0 ppm.

2.2. Laser cutting systems

Two different laser systems were used to cut the pure lithium metal. The first system employed a CW laser, while the second used a ns-pulsed laser. Both systems operated in the near-infrared (NIR) wavelength range, and their technical specifications are detailed in Table 1.

The ns-pulsed laser system was a 250 ns Q-switched fiber laser (YLP-1/100/50/50 from IPG Photonics, Oxford, MA, USA). It was coupled to a scanner head (TSH 8310 from Sunny Technology, Beijing, China) equipped with a 100 mm focal length f-theta lens (SL-1064-70-100 from Wavelength Opto-Electronic, Ronar-Smith, Singapore). With this setup, scanning speeds of up to 3 m/s could be achieved. The laser delivered an average power of up to 54 W and operated within a pulse repetition rate range of 20 to 80 kHz.

The second laser system was a single mode fiber laser emitting at a wavelength of 1070 nm (IPG Photonics, Cambridge, CA, USA) with a 2 kW maximum power. The laser featured a single-mode core with a diameter of 14 µm. The resulting focal spot diameter was 40 µm. Beam movement relative to the sample surface was achieved using a galvanometric scanner. Based on the optical configurations, the theoretical Rayleigh lengths (z_r) at the focal point were calculated to be 0.98 mm and 0.66 mm for the CW and ns-pulsed laser systems, respectively.

Table 1. Technical specifications of continuous wave and nanosecond-pulsed laser systems

Parameter	CW	ns-pulsed
Wavelength, λ (nm)	1070	1064
Max. average power, P_{avg} (W)	2000	54
Pulse repetition rate, PRR (kHz)	-	20-80
Beam quality factor, M^2	1.2	1.7
Collimated beam diameter, d_c (mm)	16.4	5.9
Focal length, f (mm)	400	100
Calculated diameter at focal point, d_0 (µm)	40	39
Rayleigh length, z_r (mm)	0.98	0.66

An air-sealed box equipped with a clamping system was used to transport the specimens from the glovebox to the laser system. During processing, the specimens were fixed in a planar position over a cutting gap. Laser processing was carried out in an argon-filled enclosure. The box was equipped with a laser window featuring a high transmissivity at NIR wavelengths. The configuration of the two lasers is similar. Fig. 2 shows a schematic representation of the laser system setup with the air-sealed box to process the lithium metal under the laser in the ambient atmosphere.

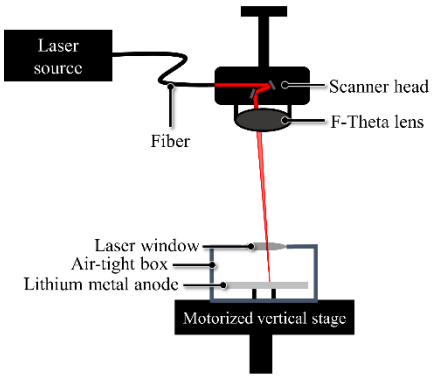

Fig. 2. Schematic representation of the laser system setup with the air-sealed box

For the ns-pulsed system the pulse energy was calculated using the average laser power (P_{avg}) and set pulse repetition rate (PRR) following the equation:

$$E = \frac{P_{avg}}{PRR} \quad (1)$$

The peak power of each pulse for the ns-pulsed laser system was calculated using the following a uniform pulse shape approximation:

$$P_{pk} = \frac{E}{\tau} \quad (2)$$

For the CW laser the power (P) value does not vary in time resulting in the condition where $P_{avg}=P_{pk}$. In order to highlight the difference of the emission mode the power values of the CW system were indicated with P.

2.3. Experimental design

In designing the experiments for laser cutting of pure lithium metal using the two laser systems, focal position (on top of the sample), and processing atmosphere (argon-filled) were kept constant. For the ns-pulsed laser system, three levels of average power (24.0, 38.5, and 53.0 W) and two levels of pulse repetition rate (50.0 and 80.0 kHz) and ten levels of scanning speed, ranging from 0.1 to 4.5 m/s, were selected. In contrast, the CW laser system was operated at the power level of 200 W, with ten scanning speeds ranging from 2.0 to 8.0 m/s. The fixed and variable parameters used for laser cutting of the pure lithium metal are summarized in Table 2.

Table 2. Design the experiments for laser cutting of pure lithium metal using continuous wave and ns-pulsed laser systems

Fixed parameters	CW	ns-pulsed
Focal position, Δz (mm)	0	0
Process atmosphere	Ar	Ar
Variable parameters		
Power	P=200 W	P_{avg} =24-54 W
Pulse repetition rate, PRR (kHz)	-	50-80
Scanning speed, v (m/s)	2.0-8.0	0.1-4.5

The results were analyzed categorically to reveal the maximum cutting speed for the chosen set of parameters. SEM images of the cuts were taken to reveal the morphology. By varying the process parameters for the two laser systems, two distinct categories of results were identified. When the scanning speed was low, the lithium metal was successfully cut by the laser. As the scanning speed increased, portions of the lithium metal remained unseparated. These samples were categorized as “No cut.” In contrast, samples that were fully separated under specific laser processing conditions were

classified as “Cut.” Fig. 3 shows the SEM images of samples processed with both the CW and ns-pulsed laser systems, categorized as “Cut” and “No cut.” The results were used to define the processability maps.

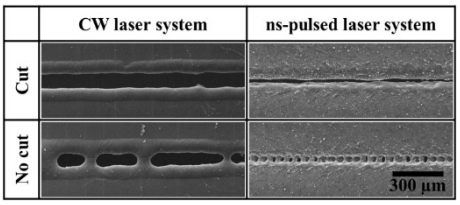

Fig. 3. SEM images of samples processed with both the CW and ns-pulsed laser systems categorized as “Cut” and “No cut”

3. Results

3.1. CW laser processability window

Fig. 4a shows the processability window of lithium metal as a function of the process parameters used with the CW laser. The maximum cutting speed achieved at 200 W laser power was 3.5 m/s. When the scanning speed was 3.5 m/s or lower, the molten material at the edges of the cutting kerf formed a dome-shaped burr. The shape of the burr is similar to that observed in (Jansen et al., 2018). With further increases in scanning speed, some parts of the material remained unseparated. Fig. 5 shows SEM images of the kerf width for samples processed at the maximum cutting speed, as well as for a sample processed at a scanning speed above this limit. These SEM images highlight the importance of scanning speed in the laser–material interaction. When the laser scanning speed exceeds a certain threshold, the input laser power is insufficient to cut through the samples.

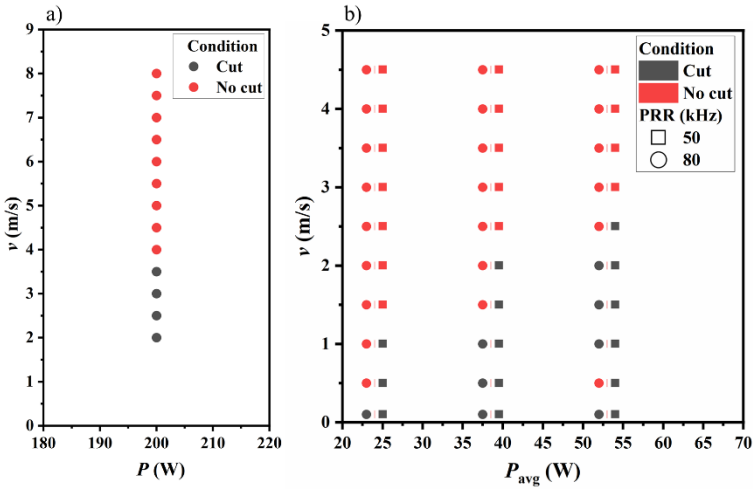

Fig. 4. Processability window of lithium metal cutting with the (a) continuous wave and (b) ns-pulsed laser systems

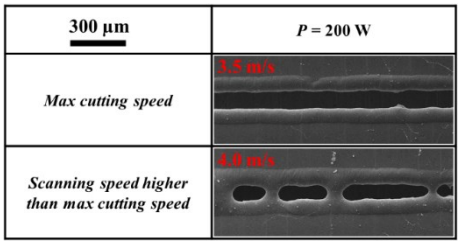

Fig. 5. SEM images of samples processed at the maximum cutting speed, and a sample processed at a scanning speed above this limit

3.2. ns-pulsed laser processability window

Fig. 4b shows the processability window for laser cutting of lithium metal based on variations in the laser's average power, PRR, and scanning speed. According to this figure, the maximum cutting speed depends not only on the laser's average

power but also on the PRR of the laser source. For all average power levels in the processability window, samples can be cut more efficiently at lower PRR levels. As shown in Equation 2, reducing the PRR increases the peak power of each pulse. This indicates that the maximum cutting speed is influenced by the peak power of the pulse. Fig. 6 presents SEM images of samples processed at the maximum cutting speed and at scanning speeds above the cutting threshold, organized by peak pulse power. As seen in this figure, increasing the peak pulse power results in a higher maximum cutting speed. Based on Fig. 6, as the peak power increases—and consequently the maximum cutting speed—the shape of the kerf width changes. At low peak power, the kerf is relatively straight and wide. At moderate peak power, the kerf width at maximum cutting speed becomes wider and wavier. However, when the peak power is further increased to its maximum, the kerf becomes narrower.

By comparing the processability windows of both laser systems in Fig. 4, the ns-pulsed laser system can cut lithium metal at speeds up to 2.5 m/s with an average power of 54 W, while the CW laser system achieves cutting speeds up to 3.5 m/s with 200 W of laser power.

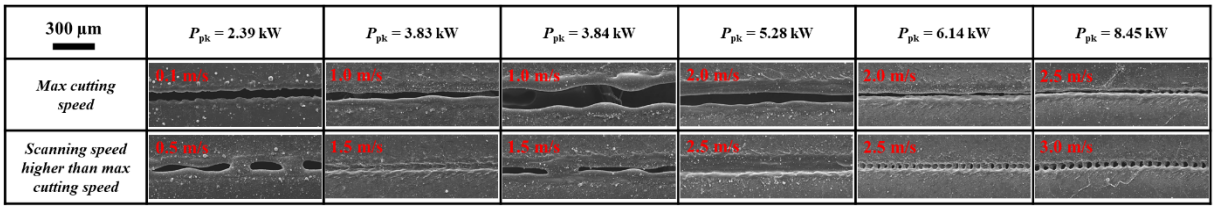

Fig. 6. SEM images of samples processed with ns-pulsed laser system organized by peak power of pulse at the maximum cutting speed and at scanning speeds above the cutting threshold

4. Conclusion

Laser cutting of lithium metal using both CW and ns-pulsed laser systems was investigated providing a preliminary view of the processing conditions. Based on the processability window for lithium metal cutting using the CW laser system, the maximum cutting speed achieved was 3.5 m/s employing 200 W. In contrast, the cutting speed in the ns-pulsed laser system depended on the peak power of individual pulses. Increasing the pulse peak power resulted in a higher maximum cutting speed. Increasing peak power changes the shape of the sample kerf width. The maximum cutting speed obtained with the ns-pulsed laser was 2.5 m/s using 54 W of average power and a PRR of 50 kHz. Based on the results of this study, the ns-pulsed laser system proved to be a more efficient solution for cutting lithium metal at higher speeds compared to the CW laser system. Future works will investigate a wider range of pulse durations along on anode materials consisting of pure Li as well as Li coated collectors.

Acknowledgements

This project has been partially funded within the national recovery and resilience (PNRR) fund under the scholarship no 38-033-16-DOT1316301-3558. The project received funding from European Commission - CINEA - European Climate, Infrastructure and Environment Executive Agency under the project "STELLAR: Safe, Sustainable & High-Throughput Production of Reliable Lithium Metal Anodes for GEN 4B/4C/5 Batteries.

References

Angeloni, C., Liverani, E., Ascari, A., Fortunato, A., 2024. Characterization and process optimization of remote laser cutting of current collectors for battery electrode production. J Mater Process Technol 324. https://doi.org/10.1016/j.jmatprotec.2023.118266

Heidari Orojloo, P., Demir, A.G., 2025. High quality remote laser cutting of polymer lithium-ion battery separator using a NIR picosecond-pulsed laser. Optik (Stuttg) 172481. https://doi.org/10.1016/j.ijleo.2025.172481

Heidari Orojloo, P., Demir, A.G., 2024. Study of burst mode for enhancing the ps-laser cutting performance of lithium-ion battery electrodes. J Laser Appl 36. https://doi.org/10.2351/7.0001417

Heidari Orojloo, P., Dib, S.A., Kriegler, J., Ballmes, H., Zaeh, M.F., Demir, A.G., 2025. Nanosecond- and picosecond-pulsed laser cutting of lithium metal anodes with copper current collector. International Journal of Advanced Manufacturing Technology. https://doi.org/10.1007/s00170-025-15885-1

Jansen, T., Blass, D., Hartwig, S., Dilger, K., 2018. Processing of advanced battery materials—laser cutting of pure lithium metal foils. Batteries 4. https://doi.org/10.3390/batteries4030037

Jansen, T., Hartwig, S., Blass, D., Dilger, K., 2019. Laser cutting of pure lithium metal anodes - Effects of atmospheric conditions. Laser Institute of America, p. 602. https://doi.org/10.2351/1.5138153

Kriegler, J., Binzer, M., Zaeh, M.F., 2021. Process strategies for laser cutting of electrodes in lithium-ion battery production. J Laser Appl 33. https://doi.org/10.2351/7.0000335

Kriegler, J., Duy Nguyen, T.M., Tomcic, L., Hille, L., Grabmann, S., Jaimez-Farnham, E.I., Zaeh, M.F., 2022. Processing of lithium metal for the production of post-lithium-ion batteries using a pulsed nanosecond fiber laser. Results in Materials 15. https://doi.org/10.1016/j.rinma.2022.100305

Kriegler, J., Hille, L., Zaeh, M.F., 2023. Picosecond-pulsed laser cutting of lithium metal substrates for post-lithium-ion battery production.

Kriegler, J., Liu, T., Hartl, R., Hille, L., Zaeh, M.F., 2023. Automated quality evaluation for laser cutting in lithium metal battery production using an instance segmentation convolutional neural network. J Laser Appl 35. https://doi.org/10.2351/7.0001213

Orojloo, P.H., Demir, A.G., 2024. Influence of electrode characteristics on the laser cutting of lithium-ion battery anodes, in: Procedia CIRP. Elsevier B.V., pp. 12–15. https://doi.org/10.1016/j.procir.2024.08.061

Shin, J., Yang, J., Lee, D., 2024. Comparison of laser processability for LiFePO4 cathode material with nanosecond and femtosecond laser. Journal of Science: Advanced Materials and Devices 9. https://doi.org/10.1016/j.jsamd.2024.100753

Thomas, F., Mahdi, L., Lemaire, J., Santos, D.M.F., 2024. Technological Advances and Market Developments of Solid-State Batteries: A Review. Materials. https://doi.org/10.3390/ma17010239